GENERAL NUMERICAL METHOD FOR THREE-DIMENSIONAL SINGULARITIES IN CRACKED OR NOTCHED ELASTIC SOLIDS

Z. P. Bažant* and L. F. Estenssoro**

INTRODUCTION

The objective of this paper is to report preliminary results of a numerical finite element study concerned with the elastic deformation field near the point where a crack front edge intersects the surface of an elastic body. The crack plane as well as the front edge are assumed to be normal to the surface. However, the numerical method, briefly outlined herein, has a general applicability to three-dimensional elastic singularities involving singular points located on stress singularity lines, such as crack edges, corners, notches, inclusion edges, etc.

The problem is of fundamental interest for the propagation of cracks intersecting a surface, and a solution is needed to assess the effect of thickness of thin sheets, plates and layers upon crack propagation. A solution of this problem has been attempted many times without success. Recently, Benthem [1] presented an analytical solution.

Problems of similar type also arise in potential theory, where they are, of course, much easier to treat. Very accurate analytical solutions of certain three-dimensional singularities in potential theory have been recently obtained by Morrison and Lewis [2], and by Keer and Parihar [3].

A general numerical method which is capable of handling any three-dimensional singularity in potential theory has been developed in reference [4]. The basic ideas of the present solution, involving the separation of variables postulated here in equations (1) and (11), and the use of finite difference or finite element method to formulate and solve a large nonlinear generalized eigenvalue problem (equation (17) in the sequel), are the same as those in reference [4].

VARIATIONAL EQUATION FOR THE EIGENSTATES

Consider a singular point, 0, located at a smooth singularity line 00' which terminates at point 0 (e.g., Figure 1). Let r, θ, ϕ be a spherical coordinate system centred at point 0, such that ray $\theta = 0$ coincides with the singularity line. It will be assumed that in the vicinity of point 0 the displacement in r, θ and ϕ directions can be expressed in the form

$$u = r^{\lambda} F(\theta,\phi) \tag{1a}$$

* Professor, Technological Institute, Northwestern University, Evanston, Ill., USA.
**Graduate Research Assistant, Northwestern University, Evanston, Ill., USA.

$$v = r^{\lambda} G(\theta,\phi) \tag{1b}$$

$$w = r^{\lambda} H(\theta,\phi) \tag{1c}$$

Substituting these expressions into the well-known differential equations of equilibrium in terms of u, v, w, it is found that the radius coordinate, r, cancels out of the equations, and the following differential equations of equilibrium in r, θ, ϕ directions in terms of functions F, G, H result:

$$X_r = (Q+2)(\lambda-1)\left[\lambda F+F+G_\theta+G\cot\theta+\frac{1}{\sin\theta}H_\phi\right]-\left[(\lambda+1)G_\theta-F_{\theta\theta}\right]$$
$$-\cot\theta\left[(\lambda+1)G-F_\theta\right]+\frac{1}{\sin\theta}\left[\frac{1}{\sin\theta}F_{\phi\phi}-H_\phi-\lambda H_\phi\right]=0 \tag{2a}$$

$$X_\theta = (Q+2)\left[\lambda F_\theta+2F_\theta+G_{\theta\theta}+G_\theta\cot\theta-\frac{1}{\sin^2\theta}G+\frac{1}{\sin\theta}H_{\theta\phi}-\frac{\cos\theta}{\sin^2\theta}H_\phi\right]$$
$$-\frac{1}{\sin\theta}\left[H_{\theta\phi}+H_\phi\cot\theta-\frac{1}{\sin\theta}G_{\phi\phi}\right]+\lambda\left[(\lambda+1)G-F_\theta\right]=0 \tag{2b}$$

$$X_\phi = \frac{1}{\sin\theta}(Q+2)\left[\lambda F_\phi+2F_\phi+G_{\theta\phi}+G_\phi\cot\theta+\frac{1}{\sin\theta}H_{\phi\phi}\right]$$
$$-\lambda\left[\frac{1}{\sin\theta}F_\phi-H-\lambda H\right]+\left[H_{\theta\theta}+H_\theta\cot\theta-\frac{1}{\sin^2\theta}H+\frac{\cos\theta}{\sin^2\theta}G_\phi\right.$$
$$\left.-\frac{1}{\sin\theta}G_{\theta\phi}\right]=0 \tag{2c}$$

where ν = Poisson ratio, $Q = 2\nu/(1-2\nu)$, and subscripts of F, G, and H denote partial derivatives; e.g., $F_{\theta\theta} = \partial^2F/\partial\theta^2$. Furthermore, substituting equations (1a - c) into the well-known expressions for spherical stress components $\sigma_{r\theta},\ldots,\sigma_{\phi\phi}$ terms of u, v, w, it is found that

$$s_{r\theta} = \frac{1}{2Gr^{\lambda-1}}\sigma_{r\theta} = \lambda G - G + F_\theta \tag{3a}$$

$$s_{\theta\theta} = \frac{1}{Gr^{\lambda-1}}\sigma_{\theta\theta} = Q\left[\lambda F+2F+G_\theta+G\cot\theta+\frac{1}{\sin\theta}H_\phi\right]+2(G_\theta+F) \tag{3b}$$

$$s_{\theta\phi} = \frac{1}{2Gr^{\lambda-1}}\sigma_{\theta\phi} = H_\theta-H\cot\theta+\frac{1}{\sin\theta}G_\phi \tag{3c}$$

$$s_{r\phi} = \frac{1}{2Gr^{\lambda-1}}\sigma_{r\phi} = \frac{1}{\sin\theta}F_\phi+\lambda H-H \tag{3d}$$

$$s_{\phi\phi} = \frac{1}{Gr^{\lambda-1}}\sigma_{\phi\phi} = Q\left[\lambda F+2F+G_\theta+G\cot\theta+\frac{1}{\sin\theta}H_\phi\right]$$
$$+2\left[\frac{1}{\sin\theta}H_\phi+G\cot\theta+F\right] \tag{3e}$$

in which G = elastic shear modulus.

Point 0 is assumed to lie at the surface of the body. Expressions (3a - e) may then be used to express surface conditions at surfaces consisting of radial rays emanating from point 0. Let $\underset{\sim}{n} = (n_\theta, n_\phi)$ represent the unit normal to the surface of the body when plotted in the (θ,ϕ)-plane, with θ and ϕ being regarded as the cartesian coordinates in such a fictitious plane; thus, $\underset{\sim}{n} \sim (d\phi/ds, -d\theta/ds)$ where s = length of boundary curve, or $n_\theta/n_\phi = -d\phi/d\theta$ where $d\phi$, $d\theta$ are increments along the boundary. The boundary condition of a free surface may be written in the (θ,ϕ)-plane in the form

$$p_r = s_{r\theta}n_\theta\sin\theta + s_{r\phi}n_\phi = 0 \tag{4a}$$

$$p_\theta = s_{\theta\theta}n_\theta\sin\theta + s_{\theta\phi}n_\phi = 0 \tag{4b}$$

$$p_\phi = s_{\theta\phi}n_\theta\sin\theta + s_{\phi\phi}n_\phi = 0 \tag{4c}$$

The differential equations (2a - c) together with the boundary conditions (4a - c) may be combined to form the following variational statement

$$\iint_A\left[X_r\delta F+X_\theta\delta G+X_\phi\delta H\right]\sin\theta\,d\theta d\phi-\int_s\left[p_r\delta F+p_\theta\delta G+p_\phi\delta H\right]ds=0 \tag{5}$$

in which s = length of the boundary of the region in the (θ,ϕ)-plane; $ds^2 = d\theta^2+d\phi^2$; A = area of this region; and variations δF, δG, δH are arbitrary continuous functions of θ and ϕ which have piece-wise continuous derivatives and satisfy all displacement boundary conditions (if any). Conversely from the fact that equation (5) must hold for any kinematically admissible functions δF, δG, δH it follows that equations (2) and (4) must be satisfied. Thus, equation (5) is equivalent to equations (2) and (4).

Equation (5) involves second derivatives of F, G, H (which are contained in the expressions for $s_{r\theta},\ldots,s_{\phi\phi}$). To be able to apply the finite element method, it is necessary to transform equation (5) to a form which involves no higher than first-order derivatives of F, G, H and of δF, δG, δH. At the same time, it is necessary that during this transformation the boundary integral in equation (5) be eliminated (or else natural boundary conditions would not be automatically satisfied when the finite element technique is used). Indeed, a transformation by Green's integral theorem, applied in the Cartesian (θ,ϕ)-plane, has been found, such that both objectives are reached simultaneously. The resulting variational equation is

$$\iint_A\left[\Phi_F\delta F+\Phi_{F_\theta}\delta F_\theta+\Phi_{F_\phi}\delta F_\phi+\Phi_G\delta G+\Phi_{G_\theta}\delta G_\theta+\Phi_{G_\phi}\delta G_\phi+\Phi_H\delta H\right.$$
$$\left.+\Phi_{H_\theta}\delta H_\theta+\Phi_{H_\phi}\delta H_\phi\right]\sin\theta\,d\theta d\phi=0 \tag{6}$$

in which the following notations are made

$$\Phi_F = [Q(1-\lambda)+2]\left[(\lambda+2)F+G_\theta+G\cot\theta+\frac{1}{\sin\theta}H_\phi\right]-2\lambda(\lambda+2)$$

$$\Phi_{F_\theta} = (\lambda-1)G+F_\theta;\quad \Phi_{F_\theta} = \frac{1}{\sin\theta}\left[\frac{1}{\sin\theta}F_\phi+(\lambda-1)H\right]$$

$$\Phi_G = \left\{(Q+2)\left[(\lambda+2)F+G_\theta+G\cot\theta+\frac{1}{\sin\theta}H_\phi\right]-2(G_\theta+F)-2\lambda F\right\}\cot\theta$$
$$-2(F_\theta-G)-\lambda(\lambda+1)G-\lambda F_\theta$$

$$\Phi_{G_\theta} = Q\left[(\lambda+2)F+G_\theta+G\cot\theta+\frac{1}{\sin\theta}H_\phi\right]+2(G_\theta+F)$$

$$\Phi_{G_\phi} = \frac{1}{\sin\theta}\left[H_\theta-H\cot\theta+\frac{1}{\sin\theta}G_\phi\right] \qquad (7)$$

$$\Phi_H = -\left\{\left[H_\theta-H\cot\theta+\frac{1}{\sin\theta}G_\phi\right]\cot\theta+2\left[\frac{1}{\sin\theta}F_\phi-H\right]+\lambda(\lambda+1)H\right.$$
$$\left.+\frac{\lambda}{\sin\theta}F_\phi\right\}$$

$$\Phi_{H_\theta} = H_\theta-H\cot\theta+\frac{1}{\sin\theta}G_\phi$$

$$\Phi_{H_\phi} = \frac{1}{\sin\theta}\left\{Q\left[(\lambda+2)F+G_\theta+G\cot\theta+\frac{1}{\sin\theta}H_\phi\right]+2\left[\frac{1}{\sin\theta}H_\phi\right.\right.$$
$$\left.\left.+G\cot\theta+F\right]\right\}$$

Alternatively, it is possible to derive equation (6) from equation (5) by means of Stokes theorem applied on a unit sphere r = 1, domain A being considered as a domain on a unit sphere. It has been checked that this gives the same result. It may be also checked that equation (6) can be transformed by means of Green's theorem (or Stokes theorem) back to equation (5).

The variational statement of the problem is: Functions F, G and H are the solution of the problem if and only if they satisfy equation (6) for any kinematically admissible variations δF, δG, δH.

Existence of variational equation (6) which contains no boundary integral indicates that natural boundary conditions (4) will be automatically fulfilled when the finite element method is used.

It is particularly noteworthy that the integrand of equation (6) is non-symmetric (and that $\Phi_F,\ldots,\Phi_{H_\phi}$ are not partial derivatives of some function Φ). This means that the variational principle cannot be written in the form of a stationary principle, $\delta W = 0$ (or minimum principle, W = min.). At first this might seem surprising for an elastic material. However, a deeper analysis indicates that it must be so. To clarify it, assume that the integrand of equation (6) is symmetric with regard to F, G, H. Then

the discrete eigenvalue problem for λ resulting from equation (6) as indicated in the sequel would have a symmetric matrix, and this would imply that all roots λ would have to be real. This is not possible because the same variational equation (equation (6)) must hold also for problems with two-material interfaces, which are known to exhibit oscillating singularities for which λ is complex. Hence, equation (6) cannot be symmetric. This contrasts with the analogous potential theory problem, for which a minimum variational principle in the (θ,ϕ)-plane does exist (see reference [4]), with the consequence that in potential theory the eigenvalues λ are always real.

The basic variational equation (equation (6)) can be also derived from the principle of strain energy, in a similar way as a minimum principle has been derived for the potential theory (equation (18) of reference [4]). The derivation is more direct but it involves certain steps which are difficult to justify without recourse to the derivation just presented. These steps involve the facts that the factor r^λ must be treated at first as an unknown function, R(r), even though r^λ is known in advance to satisfy all governing equations, and that the integral must be integrated by parts with respect to dr, leaving the question of the meaning of the boundary terms arising from integration by parts when actually no boundary intersecting the radial rays is specified in the eigenstate problem.

FINITE ELEMENT FORMULATION IN (θ,ϕ) PLANE

Compared to finite difference solutions, a finite element solution of the variational equations (6) - (7) has the tremendous advantage that stress boundary conditions are automatically implied whenever a free boundary is considered. Therefore, the finite element technique has been selected to approach the problem.

Functions F, G and H must exhibit gradient singularities at the point where they intersect the gradient singularity line (crack edge) emanating from point 0. Such functions are not suitable for numerical solution, since it is known that the rate of convergence of the finite element method with piece-wise polynomial distribution functions is $0(\sqrt{h})$ when there is crack-type singularity, while without singularity it is $0(h^2)$, h being the maximum element size. This difficulty could be avoided, e.g., by using singular finite elements near the singularity line. But a more convenient method has been proposed and used with success in reference [4]. In this method the displacements in r, θ, ϕ directions are expressed as

$$u = f^n r_1^p\, f(\theta,\phi) = r^\lambda \rho^p\, f(\theta,\phi) \qquad (8a)$$

$$v = r^n r_1^p\, g(\theta,\phi) = r^\lambda \rho^p\, g(\theta,\phi) \qquad (8b)$$

$$w = r^n r_1^p\, h(\theta,\phi) = r^\lambda \rho^p\, h(\theta,\phi) \qquad (8c)$$

in which p = exponent for the field near the singularity line; $\lambda = n+p$; $r_1 = r\rho$; ρ = any chosen smooth continuous function of θ and ϕ which is non-zero everywhere except on the singularity ray $\theta = 0$ and in the vicinity of this ray (i.e., for $\theta \to 0$) represents the distance from the ray measured on a unit sphere. Possible choices are $\rho = \theta$ or $\rho = \sin\theta$. The latter choice will be made here, and ρ will then represent the exact distance from the ray not only for $\theta \to 0$ but everywhere in the domain.

(It must be noted, however, that $\rho = \sin\theta$ cannot be used when $\theta = \pi$ is part of the domain and no line of singularity exists at $\theta = \pi$.) For crack edge, $p = 1/2$, which has been considered in all calculations presented here. (However, exponents $p = 0,1,\ldots$ are also possible [1]. It will be convenient to introduce the notations:

$$F(\theta,\phi) = \rho^p f(\theta,\phi) \qquad \left[\rho^p = (\sin\theta)^p\right] \tag{9a}$$

$$G(\theta,\phi) = \rho^p g(\theta,\phi) \tag{9b}$$

$$H(\theta,\phi) = \rho^p h(\theta,\phi) \tag{9c}$$

If the field near the singularity line varies as $\rho^{1/2}$ and p is set equal to 1/2, functions f, g, h may not exhibit any singularity at $\theta = 0$. This would make the convergence rate quadratic, $0(h^2)$. On the other hand, if components of types $\rho^{1/2}$ and ρ^0 (possibly with components of other exponents) were both present in the solution, as is indicated by Benthem's solution [1], the rate of convergence would not be quadratic, but slower than quadratic.

Choosing a finite element grid in (θ,ϕ)-plane, functions F, G, H within each finite element may be represented as

$$F = \sum_i X_i F^i, \quad F^i = \rho^p f^i \tag{10a}$$

$$G = \sum_i X_i G^i, \quad G^i = \rho^p g^i \tag{10b}$$

$$H = \sum_i X_i H^i, \quad H^i = \rho^p h^i \tag{10c}$$

in which X (i = 1,2,...,M) are the nodal values of f, g and h such that $f_k = f^{3k-2} = X_{3k-2}$, $g_k = g^{3k-1} = X_{3k-1}$, $h_k = h^{3k} = X_{3k}$, k being the mode number; and f^i, g^i, h^i are the corresponding distribution functions within the finite elements, normally chosen as polynomials in θ and ϕ. The variations of functions F, G, H and their derivatives may now be expressed as follows:

$$\delta F = \sum_j F^j \delta X_j, \quad \delta G = \sum_j G^j \delta X_j, \quad \delta H = \sum_i H^j \delta X_j \tag{11a}$$

$$\delta F_\theta = \sum_j F^j_\theta \delta X_j, \quad \delta G_\theta = \sum_j G^j_\theta \delta X_j, \quad \delta H_\theta = \sum_j H^j_\theta \delta X_j \tag{11b}$$

$$\delta F_\phi = \sum_j F^j_\phi \delta X_j, \quad \delta G_\phi = \sum_j G^j_\phi \delta X_j, \quad \delta H_\phi = \sum_j H^j_\phi \delta X_j \tag{11c}$$

Substituting equations (10a - c) and (11a - c) into equation (7), it follows that

$$\Phi_F = \sum_i \Phi^i_F X_i, \quad \Phi_{F_\theta} = \sum_i \Phi^i_{F_\theta} X_i, \ldots, \Phi_{H_\phi} = \sum_i \Phi^i_{H_\phi} X_i \tag{12}$$

in which

$$\Phi^i_F = [Q(1-\lambda)+2]\left[(\lambda+2)\rho^p f^i + (\rho^p)_\theta g^i + \rho^p g^i_\theta + \rho^p g^i \cot\theta + \frac{\rho^p}{\sin\theta} h^i_\phi\right] - 2\lambda(\lambda+2)\rho^p f^i, \quad \Phi^i_{F_\theta} = \ldots, \ldots$$

$$\Phi^i_{H_\phi} = \frac{1}{\sin\theta}\left\{\left[Q(\lambda+2)\rho^p f^i + (\rho^p)_\theta g^i + \rho^p g^i_\theta + \rho^p g^i \cot\theta + \frac{\rho^p}{\sin\theta} h^i_\phi\right] + 2\left[\frac{\rho^p}{\sin\theta} h^i_\phi + \rho^p g^i \cot\theta + \rho^p f^i\right]\right\} \tag{13}$$

Finally, substitution of equations (11) - (13) into variational (6) yields a discrete variational equation of the form

$$\sum_{j=1}^{M}\left[\sum_{i=1}^{M} k_{ij} X_j\right]\delta X_i = 0 \tag{14}$$

in which k_{ij} are stiffness coefficients expressed as follows

$$k_{ij} = \iint_A \left\{\Phi^i_F F^j + \Phi^i_{F_\theta} F^j_\theta + \Phi^i_{F_\phi} F^j_\phi + \Phi^i_G G^j + \Phi^i_{G_\theta} G^j_\theta + \Phi^i_{G_\phi} G^j_\phi + \Phi^i_H H^j + \Phi^i_{H_\theta} H^j_\theta + \Phi^i_{H_\phi} H^j_\phi\right\} \sin\theta \, d\theta d\phi \tag{15}$$

Note that the stiffness matrix $[k_{ij}]$ is non-symmetric; i.e., $k_{ij} \neq k_{ji}$ in general. The variational equation (14) must hold for any choice of δX_i (i = 1,...,M), and this requires that

$$\sum_{i=1}^{M} k_{ij} X_j = 0 \qquad (i = 1,\ldots,M). \tag{16}$$

This is a system of M linear homogeneous algebraic equations, representing an eigenvalue problem. All stiffness coeficients k_{ij}, not just the diagonal ones, depend on singularity exponent λ, and so the eigenvalue problem is of the generalized type. Furthermore, it is easy to see that k_{ij} are polynomials in λ, as well as in Poisson ratio ν (when multiplied by 1-2ν);

$$k_{ij} = k_{ij}(\lambda,\nu). \tag{17}$$

So, the generalized eigenvalue problem is a non-linear one. Various methods of numerical solution of this problem have been discussed in detail in reference [4], and method B from page 230 of reference [4] has been used here to search for the root λ. The root of smallest value (or of smallest Re(λ), in case of complex root) is of main practical interest. A method of solution when root λ is complex has been described in more detail in reference [5] in connection with another problem.

NUMERICAL RESULTS FOR CRACK EDGE TERMINATING PERPENDICULARLY AT SURFACE

The method of solution just outlined has been programmed in FORTRAN IV. The finite elements were chosen as simple four-node quadrilaterals (with 12 degrees of freedom), obtained by the mapping of a rectangle on a general quadrilateral in the (θ,ϕ)-plane. The distribution functions for F, G and H on the original rectangle have been considered as bilinear in θ and ϕ, i.e., as $a+b\theta+c\phi+d\theta\phi$. The stiffness coefficients k_{ij} were calculated by Gaussian numerical integration, using 9 integration points.

The programme is general and capable of handling various situations, such as intersections of crack edge with body surface of any orientation at an arbitrary angle, corners of any angle on the crack edge, intersection of a line notch with a surface, pyramidal notches, possibly intersecting with cracks, etc. However, so far only the case when λ is a real number has been programmed. The programme will be also capable of handling cases when complex λ must be expected, such as intersections of crack edges with two-material interfaces. But this would require conversion of the FORTRAN programme to complex arithmetic and a generalization of the root search subroutine; this has not yet been done. The results presented in the sequel are all obtained under the restriction that root λ is real.

The correctness of the programme has been checked by a number of cases of known solution. First, elementary solutions of various special cases for the domain $0 \leq \theta \leq \pi/2$, $0 \leq \phi \leq \pi$ have been substituted in equation (16). These were: (a) three rigid body rotation fields, for which $\lambda = 1$, $p = 0$; (b) the field of homogeneous uniaxial stress in the direction $\theta = \pi/2$, $\phi = 0$, for which $\lambda = p = 0$; (c) the near tip plane strain field for a mode I crack with $\nu = 0$ ($\lambda = p = 1/2$); and (d) the same for mode II crack ($\lambda = p = 1/2$). In all cases the right-hand sides of equations (16) for all i were negligibly small (compared to $\Sigma_i|k_{ij}||X_j|$). Also substituted were: (e) homogeneous strain fields, with any of the six strain components being constant ($\lambda = 1$, $p = 0$); (f) plane strain mode I and mode II near tip fields for various ν ($\lambda = p = 1/2$); (g) antiplane mode III near-tip field ($\lambda = p = 1/2$); these fields cannot satisfy equations (16) for the nodes on the body surface, but they must satisfy them for all other nodes, and this was found to be true.

The programme was then applied to analyzing the field near the terminal point 0 of a crack whose plane and edge are normal to halfspace surface. Because of symmetry, it is sufficient to consider the domain $0 \leq \theta \leq \pi/2$, $0 \leq \phi \leq \pi$ (Figure 1), which has a rectangular shape in the (θ,ϕ) plane. The stress boundary conditions on crack surface ($\phi = 0$) and on half-space surface ($\theta = \pi/2$) are automatically satisfied, the boundary condition at $\theta = 0$ (pole) are irrelevant and were considered also as a free boundary, and the boundary conditions on the side $\phi = \pi$ (symmetry plane) must ensure a statically determinate support of the body and at the same time properly reflect the symmetry and antisymmetry properties of displacement field in the plane $\phi = 0$ that is normal to crack front edge. These conditions are achieved, in case of mode I crack, by imposing at the nodes with $\theta = \pi$ the condition $w = 0$ or $h = 0$, and only this case has been considered thus far in the solution of non-trivial cases. In case of mode II crack, antisymmetry of displacements in the plane $\phi = 0$ with respect to crack front edge requires that $u \sin\theta = v \cos\theta = 0$ for $f \sin\theta = g \cos\theta = 0$ at $\phi = \pi$; and in case of mode III crack, antisymmetry of displacements in the plane $\phi = 0$ with respect to the ray $\theta = \phi = \pi/2$ requires that $u \cos\theta - v \sin\theta = 0$ or $f \cos\theta - g \sin\theta = 0$ at $\theta = \pi$.

To obtain a picture of accuracy and convergence, root λ was first solved for $\nu = 0$, in which case the solution is known to be $\lambda = 0.5$. Grids of increasing numbers of finite elements, with N = 18, 32, 72 and 128 elements (and 84, 135, 273 and 459 degrees of freedom), were used. In the (θ,ϕ)-plane all elements were rectangular and identical; the subdivisions of the region in the θ- and ϕ-directions were 3 x 6, 4 x 8, 6 x 12, and 8 x 16. The results of these calculations are given in Figure 3; see line $\nu = 0$. For the finest grid used (128 elements, 459 simultaneous equations), the computed value of the root was 0.5097, which is still 1.9% in error. This indicates that for accurate calculation of λ a finer grid and more complicated finite elements will be required. Work in this direction is in progress.

Nevertheless, even from the results for the relatively crude grids used thus far, interesting results can be extracted if the practical convergence is studied more carefully. It is well known that ordinary finite element method exhibits quadratic convergence, i.e., it has error of the order $O(h^2)$, h being the maximum size of the finite element, provided that there are no singularities within the domain. Functions f, g, h and their gradients are nonsingular, and so the convergence should be also quadratic in the present case. Noting that $h^2 \sim 1/N$, it follows that error $\approx k/N$ where k = constant and N = number of finite elements. This relation should hold accurately when N is sufficiently large. Hence, $\log(\text{error}) = \log(\lambda - 0.5) = \log k - \log N = \log k - 2\log\sqrt{N}$, which indicates that the plot of log(error) versus $\log\sqrt{N}$ must become a straight line of slope -2 when N is sufficiently large. This plot is shown for $\nu = 0$ in Figure 2, and it is seen that the plot is indeed a straight line, and that the slope of this line is exactly -2.0. Thus, for $\nu = 0$ the present formulation seems to follow a systematic pattern of quadratic convergence already for rather crude grids. This can be used to advantage in extrapolating the convergence pattern and estimating the results for $N \to \infty$.

Thus, expecting that $\lambda - \lambda_{exact} = k/N$, the numerical results for various values of ν obtained with various numbers of finite elements may be used to construct a plot of λ versus 1000/N (Figure 3). Again, for quadratic convergence these plots would have to be straight lines for a sufficiently large N. According to Figure 3 this seems indeed to be true. Therefore, straight lines (regression lines) have been passed in Figure 3 to obtain estimates of the values for $N \to \infty$, i.e., estimates of the exact solution. In case of $\nu = 0$, the point $N \to \infty$ falls exactly in 0.5. However, calculations with much finer grids will be required to make definite conclusions about the values for $N \to \infty$. Especially, caution is necessary in view of the fact that the estimates for $N \to \infty$ significantly deviate from Benthem's solution [1] (Figure 3). According to Benthem, the field in equation (8) with $p = 1/2$ is not the complete solution, unless $\nu = 0$, and components of the form of equation (8) but with $p = 0$ and $p = 1$ also significantly participate in the exact solution. If this were indeed true, the convergence of the present method could not be quadratic, $O(h^2)$, but slower; then, for high N the points in Figure 3 would have to begin deviating from a straight line. Based on the crude grids used thus far, this possibility cannot be discounted. If p were set equal to 0 rather than 1/2, the convergence rate would then be $O(\sqrt{h})$; accordingly, the results would have to give a straight line in a plot of λ versus $N^{-1/4}$, regardless of whether components with $p \geq 1$ are present. This case must be examined when results for very fine grids become available.

The solutions of λ for $N \to \infty$ obtained in this manner for various ν are shown in Figure 4, along with the results for various grids. Also shown

in Figure 4 is the recent approximate analytical solution by Benthem [1].

For values of ν which exceed 0.4, the root search subroutine converged poorly or not at all. In this regard, it is noteworthy that the lines for a chosen number N of elements turn sharply upwards as ν exceeds 0.4. The search for root λ may be gometrically interpreted as intersection of the line of solution for constant N with the vertical line ν = const. For $\nu > 0.4$ either the intersections occur at very small angles or (for low N) no intersection seems to exist. To circumvent this difficulty, equation (16) may be considered as an eigenvalue problem for ν at a fixed λ. Then the solution represents an intersection of the line of constant N with the horizontal line λ = const. This intersection is at large angle and appears to exist for ν-values well over 0.4. So, the convergence should be rapid and, indeed, this was found to be the case. The convergence should again be quadratic, and so the plots of ν versus 1000/N at constant λ should be straight lines. Numerical results have confirmed it. Passing straight regression lines, similarly to Figure 3 (but for λ = const.), the extrapolated values for $N \to \infty$ have been determined. These values are also plotted in Figure 4, and the solution is extended to ν-values beyond 0.4. However, when ν becomes very close to 0.5, the present formulation breaks down because the value of Q increases without bounds. A special programme would have to be written for ν close to 0.5.

However, in view of the Benthem's solution, the same cautious view as expressed earlier must be adopted with regard to extrapolations to ∞. It may also be noted that the line for $N \to \infty$ in Figure 4 seems to be aiming into the point $\lambda = 1$ and $\nu = 0.5$. Although this point has been given by Benthem [1] as a point of exact solution, this would mean that there would be no singularity for $\nu = 0.5$, and this would be in disagreement with Benthem's experimental study which indicated that for $\nu = 0.5$ the singularity exponent λ should be much less than 1 and closer to 0.5.

CONCLUSION

A general numerical method for determination of three-dimensional singular fields in elasticity has been presented and verified. However, it would be premature to make conclusions on the basis of the numerical examples presented here.

ACKNOWLEDGEMENT

Thanks are due to Leon M. Keer, Professor at Northwestern University and co-director of the project, for his stimulating discussions and valuable suggestions during the progress of this work. The writers are also obliged to Jan P. Benthem, Professor at Delft University of Technology, for pointing out the possibility of simultaneous appearance of components of various p. S. S. Kim, R. J. Krizek and W. Thonguthai are thanked for helping to check some of the calculations, alternative approaches, and subroutines.

Support by the U.S. Air Force Office of Scientific Research under Grant No. AFOSR 75-2859 is gratefully acknowledged.

APPENDIX - NOTE ON THE ANGLE OF PROPAGATING CRACK

From the practical point of view, the case of a propagating crack is of main interest. There is no reason why the angle β of the crack front edge with the surface should have the value of $\pi/2$ which has been considered in the preceding analysis.

There exist certain simple physical restrictions for the solution of a propagating crack: (a) the flux E_0 of energy into the moving crack front edge per unit length of edge must be finite and non-zero because the surface energy γ is finite and non-zero, and (b) the flux E_1 of energy into any point on crack front, including the surface point 0, must be zero, because the trace of the surface point 0 as it moves is a line, and a line can be associated only with a negligible amount of additional surface energy.

The first condition requires that $E_0 = \oint_L \sigma_{ij}(\partial u_i/\partial x) r_1 d\phi$ where r_1, ϕ is a polar coordinate system in a plane normal to crack front edge, L is a circle of radius r_1 in this plane centred around the edge, x is the direction of crack propagation, σ_{ij} is the cartesian stress tensor, and u_i are cartesian displacements. Noting that $u_j \sim r_1^p$, $\partial u_j/\partial x \sim r_1^{p-1}$, $\sigma_{ij} \sim r_1^{p-1}$ it follows that $E_0 \sim r_1^{2p-1}$, and for this to be finite as $r_1 \to 0$, it is necessary that $2\,\mathrm{Re}(p) - 1 = 0$ or $\mathrm{Re}(p) = 1/2$, as is well known.

The second condition (b) requires that $E_1 = \oint_\Omega \sigma_{ij}(\partial u_j/\partial x) d\Omega = 0$ where σ_{ij} = cartesian stress tensor, u_j = cartesian displacements, x = coordinate in the direction of crack extension, Ω = surface of a sufficiently small sphere with centre at point 0. Noting that $u_j \sim r^\lambda$, $\partial u_j/\partial x \sim r^{\lambda-1}$, $\sigma_{ij} \sim r^{\lambda-1}$ and $d\Omega = r^2 \sin\theta\, d\theta d\phi$, it follows that $E_1 \sim r^{2\lambda}$, and for this to be zero as $r \to 0$ it is necessary that

$$\mathrm{Re}(\lambda) > 0. \tag{18}$$

Furthermore, consider condition (a) and assume that the value of surface energy of crack extension, γ, is constant. Then the value of the stress intensity factor, K, must be also constant along the crack front edge, $\theta = 0$. Factor K is proportional to the displacements at a chosen fixed distance r_1 from the edge $\theta = 0$; i.e., $K \sim u \sim r^{\lambda-p} r_1^p f(\theta,\phi)$. Along the edge $\theta = 0$, only the value of r varies while r_1 and f do not. Thus, a constancy of K along the crack front edge requires that $\lambda - p = 0$ ($\mathrm{Re}(p) = 1/2$). So, it has to be concluded that

$$\mathrm{Re}(\lambda) = 1/2 \tag{19}$$

must hold for the terminal surface point of a crack that propagates.

In consequence, the most relevant problem is to determine the value of angle β which the crack front edge must form with the surface in order to yield $\lambda = 1/2$. This should be the main objective of further investigations.

REFERENCES

1. BENTHEM, J. P., "Three-Dimensional State of Stress at the Vertex of a Quarter-Infinite Crack in a Half-Space", Report No. 563, Laboratory of Engng. Mechanics, Delft University of Technology, Netherlands, September, 1975.

2. MORRISON, J. A. and LEWIS, J. A., "Charge Singularity at the Corner of a Flat Plate", SIAM J. Appl. Math., 31, 1976, 233-250.
3. KEER, L. M. and PARIHAR, K. S., "Singularity at the Corner of a Wedge-Shaped Punch or Crack", Northwestern University, August 1976 (private communication).
4. BAŽANT, Z. P., "Three-Dimensional Harmonic Functions Near Termination or Intersection of Gradient Singularity Lines: A General Numerical Method", Int. J. Engng. Sci., 12, 1974, 221-243.
5. ACHENBACH, J. D., BAŽANT, Z. P. and KHETAN, R. P., "Elastodynamic Near Tip Fields for a Crack Propagating Along the Interface of Two Orthotropic Solids", Int. J. Engng. Sci., 14, 1976, 811-818.

ADDENDUM

In subsequent work, the question of the proper value of the exponent p of distance $\rho = \sin\theta$ from the singularity line has been studied more carefully. Let $(r\rho)^p$ be the term of lowest exponent in the field near the singularity line ($\rho = \theta = 0$). For crack edge singularity, the lowest p corresponding to deformed states is p = 1/2. However, for rigid body rotations in the neighborhood of the singularity line, one has p = 0. For p = 0, the term $(r\rho)^p$ does not cause any singularity as $p \to 0$ (or $\theta \to 0$) at finite fixed r. However, this may cause gradient singularity of the type θ^{p-1} or θ^{-1} for $r \to 0$, which is more severe than the singularity $\theta^{-1/2}$ associated with the planar near tip field of a crack. That terms of θ^{-1} should indeed be present is indicated by Benthem's solution [1].

Therefore, all finite element solutions were rerun with p = 0. The resulting values of λ were plotted versus $1000/N^{m/2}$ for various chosen values of m, and the convergence rate exponent m which gives the best straight-line fit, as indicated by the sum of square deviations, was selected. This exponent varied between m = 1.7 and m = 1.9 for all ν. Furthermore, plotting $\log(\lambda - 0.5)$ versus $\log\sqrt{N}$ for $\nu = 0$ (and p = 0), the convergence rate was obtained as m = 1.9. Obviously, the convergence should not have been quadratic ($m \neq 2$) (since the gradients of F, G and H exhibit singularities at $\theta = 0$), but it is of interest that the exponent m is so close to 2, giving still quite a rapid convergence. Using the plots of λ versus $1000/N^{m/2}$ for the optimum value of m, the λ-values have been extrapolated for $N \to \infty$. In these plots the points fell on straight lines just about as closely as the points in Figure 3, but the lines were more steeply inclined than those in Figure 3. The extrapolated values for $N \to \infty$ values agreed within about 0.4% with Benthem's values for all ν between 0 and 0.48. This *confirms the Benthem's solution* as well as the present one as sufficiently accurate.

The choice p = 1/2 in previous computations (Figures 2-4) was motivated by the fact that the term $(\rho\theta)^{1/2}$ is dominant at $\theta \to 0$ and finite r. However, the results just reported show the choice p = 1/2 was inappropriate. This can be also deduced as follows. Let $u \sim r^\lambda \theta^p F(\theta,\phi)$ be the term of lowest p present at $r \to 0$ for the exact solution ($\rho = \sin\theta \approx \theta$), and assume that a different exponent $p^* \neq p$, is considered instead of p for the numerical solution, i.e., $u \sim r^\lambda \theta^{p^*} F^*(\theta,\phi)$. Then, for the stress components, $\sigma_{ij} \sim \partial u/\partial\theta \sim r^\lambda \theta^{p-1} F(\theta,\phi)$ for the exact solution and $\sigma_{ij} \sim r^\lambda \theta^{p^*-1} F(\theta,\phi)$ for the numerical solution. Equating these two expressions for σ_{ij}, one has

$$F^*(\theta,\phi) = \theta^{p-p^*} F(\theta,\phi). \qquad (20)$$

In previous computations (Figures 2-4), $p^* = 1/2$ while p = 0 exists, giving $F^*(\theta,\phi) = \theta^{1/2} F(\theta,\phi)$. Obviously, $F^*(\theta,\phi) \to \infty$ as $\theta \to 0$, and so $F^*(\theta,\phi)$ can

in no way be adequately represented numerically. If $p^* = 0$, then $p^* - p = 0$ for the term which prevails at $\theta \to 0$, giving $F^*(\theta,\phi) = F(\theta,\phi)$ which ought to be a bounded smooth function that can be adequately represented numerically.

A less severe singular term with p = 1/2 is always present at the same time, of course. For this term, $F^*(\theta,\phi) = \theta^{1/2} F(\theta,\phi)$; $F^*(\theta,\phi)$ is still bounded and acceptable for numerical representation, but because $\partial F^*(\theta,\phi)/\partial\theta$ tends to infinity as $\theta \to 0$, the accuracy of representation will be worse, causing the convergence rate to become less than quadratic.

Therefore, a quadratic convergence cannot be achieved with the present method of analysis.

Because the slope of $F^*(\theta,\phi)$ in the θ direction tends to infinity as $\theta \to 0$, it seems appropriate to refine the grid step $\Delta\theta$ as θ decreases. Irregular rectangular networks in which $\Delta\phi$ was constant and in which $\Delta\theta$ was refined so as to keep $\Delta\theta$ roughly equal $(\sin\theta)\,\Delta\phi$, have been tried, using same numbers of divisions in both θ and ϕ directions. Curiously, however, the results were not any better than those for regular grids; the plots of λ versus $1000/N^{m/2}$ had about the same inclination. But the extrapolated λ-values for $N \to \infty$ agreed again with simple check cases and with Benthem's solution within a 0.4% error (N=121 being the finest grid used).

As an additional check, the case of a right-angle corner on the front edge of a plane crack was solved. The solution for this case was obtained in equation (39) of reference [4] as $\lambda = 0.296$ for any ν and more accurately as $\lambda = 0.2966$ in references [2] and [3]. The extrapolated value of λ for $N \to \infty$ agreed with this within 0.2% error for $\nu = 0$ and $\nu = 0.3$, using N = 128 as the finest grid.

Presently, computations of λ are in progress for cracks whose plane is normal to the half-space surface but the front edge forms angle $\beta \neq \pi/2$ with the surface. Preliminary results indicate that λ decreases (below Benthem's values for $\beta = \pi/2$) as β exceeds $\pi/2$. The practically most important case $\lambda = 1/2$ is obtained for about $\beta = 101°$ if $\nu = 0.3$. This solution will be reported separately.

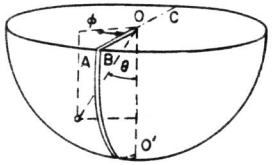

Figure 1 Geometry of the Crack Intersecting a Surface, in Spherical Coordinates

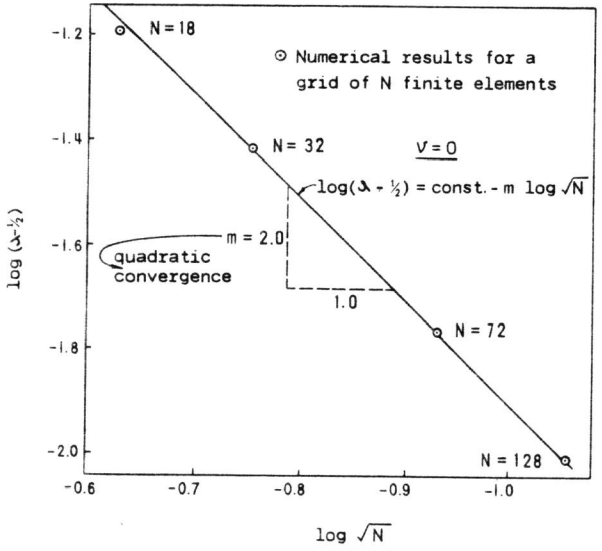

Figure 2 Determination of the Rate of Convergence with Increasing Number of Elements

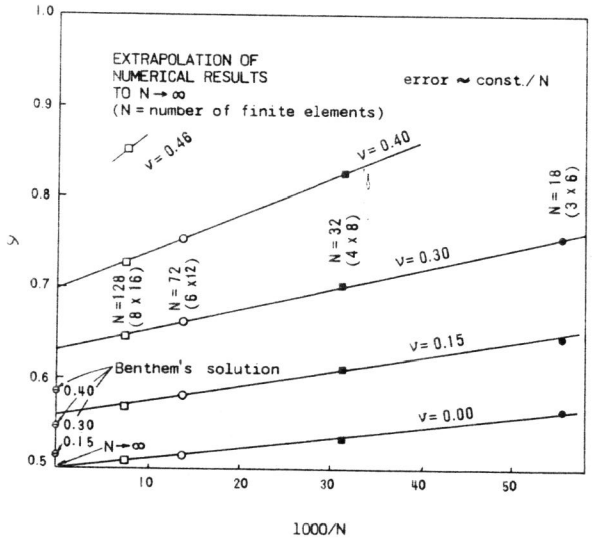

Figure 3 Tentative Extrapolation of Numerical Results to Infinite Number of Elements

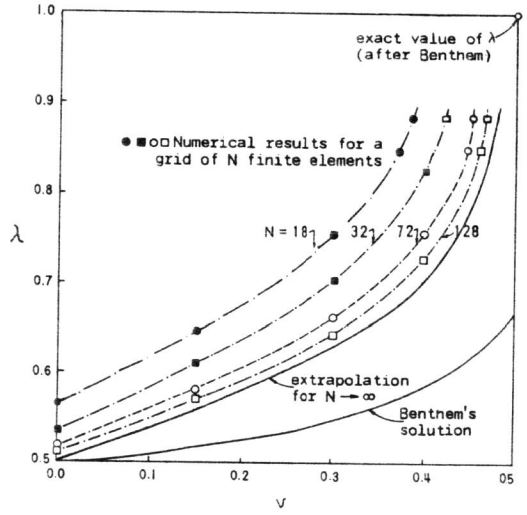

Figure 4 Singularity Exponent λ for Various Values of Poisson Ratio